Two-nucleon model calculation of (p,π^-) spectra for calcium isotopes

Naoko Nose,[1] Kenji Kume,[2] and Hiroshi Toki[1]
[1]*Research Center for Nuclear Physics, Osaka University, Ibaraki 567, Japan*
[2]*Department of Physics, Nara Women's University, Nara 630, Japan*
(Received 14 August 1995)

We have calculated the (p,π^-) spectra for calcium isotopes based on a two-nucleon pion-production model. In the near-threshold region, the observed selective excitation of high-spin states is well explained. The experimental data are reproduced within a factor of 2–3. In the higher-energy region, our calculation predicts a pronounced selectivity for stretched two-particle–one-hole high-spin states. [S0556-2813(96)04905-9]

PACS number(s): 21.60.Cs,25.40.Qa,27.40+z

I. INTRODUCTION

The prominent feature of the near-threshold (p,π^-) reaction is the highly selective excitation of the low-lying high-spin states. In (p,π^-) reactions, large momentum and large angular momentum transfer are involved and only a single two-body process, $p+n\rightarrow pp+\pi^-$, contributes. Because of these, the (p,π^-) spectra exhibit a somewhat simpler structure than (p,π^+): low-lying high-spin states with predominant two-particle–one-hole (2p-1h) structure are selectively excited and also the asymmetry for these transitions takes on quite similar patterns irrespective of the target nuclei [1–5].

Brown *et al.* have made zero-range plane-wave calculation [6] and have shown that the overall feature of the relative reaction strengths for the near-threshold (p,π^-) reactions for $f_{7/2}$-shell nuclei are well explained. Encouraged by their results, one of the authors (K.K.) has carried out a finite-range distorted-wave Born approximation (DWBA) calculation of the differential cross section and the asymmetry for the stretched-state transitions, $^{88}\mathrm{Sr}(p,\pi^-)$ and $^{48}\mathrm{Ca}(p,\pi^-)$, and has shown that the two-body process $p+n\rightarrow pp(^1S_0)+\pi^-$ dominates, which is due to the large momentum transfer to the nucleus [7–9]. At the same time, it is shown that the large angular momentum transfer to the nucleus is well accommodated by the large orbital angular momentum of the final 2p-1h state. For the final $pp(^1S_0)$ channel, the asymmetry takes a large positive value mainly due to pion distortion effects, resulting in the characteristic pattern of the asymmetry for the high-spin states [10]. These results seem to justify the zero-range assumption of Brown *et al.* [6] for the stretched-state transitions. Although they succeeded in reproducing the relative population in the (p,π^-) reactions for several $f_{7/2}$-shell nuclei, they did not calculate the absolute value of the (p,π^-) cross section because of the plane-wave approximation. In order to simulate the pion distortion effect, they introduced a radial cutoff for the overlap integrals and the cutoff radius was determined so as to fit the angular distribution of the pions in the stretched-state transitions. They also used the zero-range approximation for the two-body pion production operators. To examine the validity of these approximations, a more elaborate DWBA treatment is necessary.

In the present work, we have carried out calculations assuming the conventional two-nucleon mechanism for pion production in the framework of the DWBA for the (p,π^-) spectra of calcium isotopes and compared them with the experimental data up to absolute normalization. It is shown that the observed selective excitation of high-spin states is well explained in the near-threshold region. The absolute values of the cross sections are larger than the experiment by about a factor of 2–3 at $T_p=206$ MeV and are somewhat smaller than the experiment at $T_p=166$ MeV. Though we cannot reproduce the precise absolute values of the cross section, we succeeded in explaining the overall features of the (p,π^-) spectra without introducing adjustable parameters to fit the (p,π^-) data.

So far, theoretical and the experimental works have been mainly concerned with the near-threshold region. Considering the availability of high quality proton beam at 400 MeV in RCNP Osaka, it is interesting to study the energy dependence of the (p,π^-) spectra. Since normalization factors of 2–3 were necessary to explain the absolute values of the cross sections in the near-threshold region, we could not use our model to predict the precise absolute values of the cross section. Our aim here is the prediction of the overall trends of the (p,π^-) spectra at high energy. For the dominant transitions to high-spin states, the calculated reaction cross section takes maximal values around the proton incident energy $T_p\sim200$ MeV. In the higher-energy region, our calculation predicts a pronounced selectivity for the stretched 2p-1h high-spin states.

In Sec. II, we give a brief description of the two-nucleon model adopted in the present work. The results of two-body

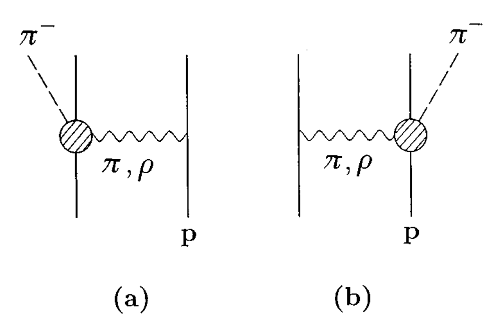

FIG. 1. Two-nucleon pion-production processes assumed in the calculation.

DWBA calculations are shown and are discussed in Sec. III. We summarize the results in Sec. IV.

II. TWO-NUCLEON MODEL

We assumed the two-nucleon pion-production processes as in Fig. 1. We have taken into account the p-wave rescattering diagrams with π and ρ exchange. In the near-threshold region ($T_p \leqslant 300$ MeV), we also take into account the s-wave rescattering contribution. The amplitude for the p-wave rescattering diagrams is given by

$$M_{ij}^{(p)} = \frac{f_\pi^*}{m_\pi}(\mathbf{S}_j \cdot \mathbf{k})(-)^\alpha \mathbf{T}_j^{-\alpha}[V_\pi(q) + V_\rho(q)]D_\Delta, \quad (1)$$

where D_Δ is the Δ propagator and V_π and V_ρ are given by

$$V_\pi(q) = \frac{f_\pi(q^2) f_\pi^*(q^2)}{m_\pi^2}(\boldsymbol{\sigma}_i \cdot \mathbf{q})(\mathbf{S}_j^\dagger \cdot \mathbf{q})(\boldsymbol{\tau}_i \cdot \mathbf{T}_j^\dagger) \times \frac{-1}{(2\pi)^3(\mathbf{q}^2 - q_0^2 + m_\pi^2)} \quad (2)$$

and

$$V_\rho(q) = \frac{f_\rho(q^2) f_\rho^*(q^2)}{m_\rho^2}(\boldsymbol{\sigma}_i \times \mathbf{q})(\mathbf{S}_j^\dagger \times \mathbf{q})(\boldsymbol{\tau}_i \cdot \mathbf{T}_j^\dagger) \times \frac{-1}{(2\pi)^3(\mathbf{q}^2 - q_0^2 + m_\rho^2)}. \quad (3)$$

Here, we use the static form of the πNN vertex. The transition spin and isospin operators are denoted by **S** and **T**, respectively. We assume the following form of the form factors:

$$f_{\pi,\rho}(q^2) = f_{\pi,\rho}\frac{\Lambda_{\pi,\rho}^2 - m_{\pi,\rho}^2}{\Lambda_{\pi,\rho}^2 - q_0^2 + \mathbf{q}^2},$$
$$f_{\pi,\rho}^*(q^2) = f_{\pi,\rho}^*\frac{\Lambda_{\pi,\rho}^{*2} - m_{\pi,\rho}^2}{\Lambda_{\pi,\rho}^{*2} - q_0^2 + \mathbf{q}^2}. \quad (4)$$

For the s-wave rescattering diagrams, we use the phenomenological interaction Hamiltonian of Koltun and Reitan [11]. The corresponding s-wave rescattering amplitude is given by

$$M_{ij}^{(s)} = 8\pi\frac{f_\pi(q^2)}{m_\pi}(\boldsymbol{\sigma}_i \cdot \mathbf{q})\left[\frac{\lambda_1}{m_\pi}(-)^\alpha \tau_i^{-\alpha} - \frac{\lambda_2}{m_\pi^2}\frac{q_0 + \omega_k}{2} \times i(\boldsymbol{\tau}_i \times \boldsymbol{\tau}_j)^{-\alpha}(-)^\alpha\right] \times \frac{-1}{(2\pi)^3(\mathbf{q}_0^2 + m_\pi^2)}, \quad (5)$$

and we assume the off-shell extrapolation of the coupling strengths due to Maxwell *et al.* [12]:

$$\lambda_1(t) = -\frac{1}{2}m_\pi\left(a_{\mathrm{sr}} + a_\sigma\frac{m_\sigma^2}{m_\sigma^2 - t}\right), \quad (6)$$

$$\lambda_2(t) = \lambda_2\frac{m_\rho^2}{m_\rho^2 - t}, \quad (7)$$

where t is the four momentum transfer in the πN t channel. We adopt the values $a_{\mathrm{sr}} = -0.23 m_\pi^{-1}$, $a_\sigma = 0.22 m_\pi^{-1}$, and $m_\sigma = 4.2 m_\pi$ [12]. The effects of the two-nucleon correlation are taken into account phenomenologically according to the method of Oset and Weise [13] with a correlation function of the form

$$\Omega(r) = 1 - j_0(m_c|\mathbf{r}_1 - \mathbf{r}_2|), \quad (8)$$

and we take the ω meson mass for m_c. The $V_{\pi,\rho}(q)$ in Eqs. (2) and (3) are replaced by $V_{\pi,\rho}^c$ as

$$V_{\pi,\rho}(q) \to V_{\pi,\rho}^c(q) = \int e^{i\mathbf{q}\cdot\mathbf{r}} V_{\pi,\rho}(\mathbf{r})\Omega(r) d\mathbf{r}. \quad (9)$$

The numerical values of the input parameters are the same as those used in Ref. [7]. The amplitudes $M_{ij}^{(p)}$ and $M_{ij}^{(s)}$ in Eqs. (1) and (5) are expanded into multipole series and these are sandwiched by the initial and final nuclear wave functions and the proton and the pion distorted waves.

III. RESULTS OF THE CALCULATION

Using the model described in Sec. II, we calculate the (p,π^-) reaction cross sections for calcium isotopes. To calculate the 2p-1h amplitudes, we adopt the $f_{7/2}$ shell-model wave functions by Kutschera *et al.* with the effective two-body matrix elements ^{42}Sc-INT [14]. These wave functions were used also by Brown *et al.* for their simple plane-wave Born approximation (PWBA) calculations of (p,π^-) reactions [6]. The distorted waves of the incident proton are generated by a nonrelativistic proton-nucleus optical potential with the parameters given by Nadasen *et al.* [15] for $T_p = 166$ and 206 MeV. For $T_p = 334$ and 362 MeV, we use the parameters in Refs. [16] and [17], respectively. We use a nonrelativistic optical potential with parameters determined from the fit to the elastic scattering data. We calculate the pion distorted waves with the pion-nucleus optical potential. We assume the form of optical potential by Stricker and co-workers [18–20]. This potential is constructed to describe low-energy pion-nucleus scattering and hence we have to extrapolate the potential parameters to higher energies. We use impulse values for the s- and p-wave parameters $b_{0,1}$ and $c_{0,1}$. For the absorption parameters B_0 and C_0, we adopt the values determined phenomenologically by Gmitro *et al.* [21]. This optical potential gives a good reproduction of the pion scattering data.

In Fig. 2, we show the calculated (p,π^-) cross section averaged by the Gaussian function with $\Gamma_{\mathrm{FWHM}} = 0.3$ MeV at $T_p = 206$ MeV and 30° and these are compared with the experimental data of IUCF [5]. The theoretical values are multiplied by a factor of 0.3 to compare with the experiments. The present results are similar to those of PWBA calculations by Brown *et al.* [6] and explain the overall feature of the reaction spectra of the (p,π^-) reactions. In the plane-wave calculation of Brown *et al.*, they cut off the radial integral in order to simulate strong pion absorption. They used a cutoff radius $R_{\mathrm{cut}} = 3.3$ fm, which gives the best reproduction of the angular distribution of the ^{48}Ca(p,π^-) reaction. They also used the zero-range approximation for the two-body pion-production operators, and hence they only calculated the relative strength of the (p,π^-) spectra. In our calculation, we take into account distortion effects and cal-

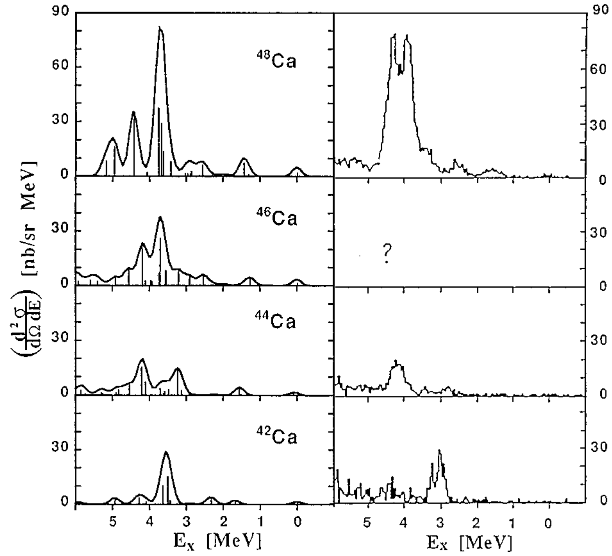

FIG. 2. Comparison of the theoretical results of (p,π^-) spectra with the experimental data of Ref. [5] at $T_p=206$ MeV and 30°. The individual final states are represented by lines and the curves are Gaussian averaged with $\Gamma_{\mathrm{FWHM}}=0.3$ MeV. The theoretical results are multiplied by factor of 0.3 to compare with experiment.

culate the absolute values of the reaction cross sections. As seen in Fig. 2, the theoretical results are found to be larger by about a factor of 2–3 for the calcium isotopes at $T_p=206$ MeV. For ^{48}Ca, the $(\frac{19}{2}^-)_1$ state at $E_x=4.38$ MeV is rather more weakly populated than the $(\frac{15}{2}^-)_2$ state at $E_x=3.96$ MeV. In Fig. 3, the results at $T_p=166$ MeV and 45° are shown and are compared with the experimental data [5]. Although the absolute values of the theoretical results are somewhat smaller than the experiment, the agreement between theory and experiment is satisfactory. The two levels, the $(\frac{19}{2}^-)_1$ state at $E_x=4.38$ MeV and the $(\frac{15}{2}^-)_2$ state at $E_x=3.96$ MeV, are strongly excited because of the momentum- and angular-momentum-matching conditions. The calculated relative strengths of these high-spin states are found slightly larger in this case than those calculated by Kume with another pion optical potential [8]. Though we could not reproduce the precise values of the absolute values of the cross sections, we would like to emphasize that the overall features of the (p,π^-) spectra are explained without introducing any adjustable parameters to fit the (p,π^-) spectra.

Considering the availability of good quality proton beams up to 400 MeV at RCNP in Osaka University, we think it interesting to extend our calculation to higher energies. Since normalization factors of 2–3 were necessary to explain the absolute values of the cross sections in the near-threshold region, we could not use our model to predict the precise absolute values of the cross section. Our aim here is to see the overall trends of the (p,π^-) spectra around the energy region near and above the delta resonance. In Fig. 4, the results of the cross sections at 20° are shown for ^{48}Ca$(p,\pi^-)^{49}$Ti at various incident proton energies. The low-lying high-spin states, $(\frac{15}{2}^-)_2$ at $E_x=3.96$ MeV and $(\frac{19}{2}^-)_1$ at $E_x=4.38$ MeV, are strongly excited for the entire energy range. The $(\frac{19}{2}^-)_1$ state at $E_x=4.38$ MeV is strongly populated at the higher-energy region. The absolute values of the cross section take maximal values around $T_p\sim200$ MeV. The pion production cross sections leading to the high-spin states $(\frac{15}{2}^-)_2$ and $(\frac{19}{2}^-)_1$ at 20° are shown in Fig. 5. We ex-

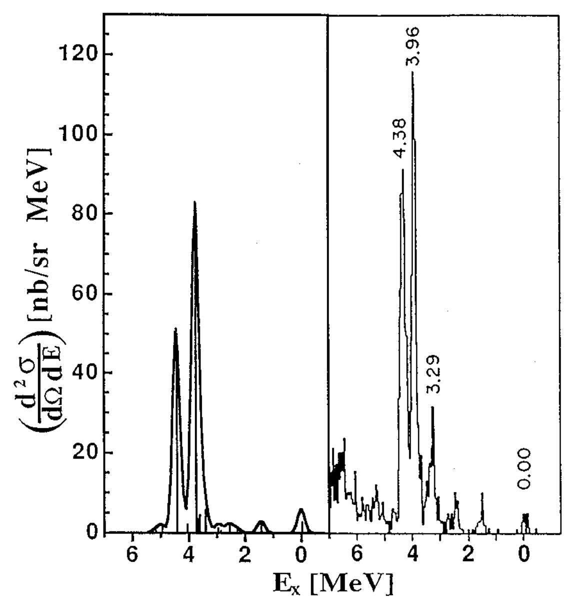

FIG. 3. Comparison of the theoretical (p,π^-) spectra with the experimental data of Ref. [5] at $T_p=166$ MeV and 45°. The individual final states are represented by lines and the curves are Gaussian averaged with $\Gamma_{\mathrm{FWHM}}=0.3$ MeV.

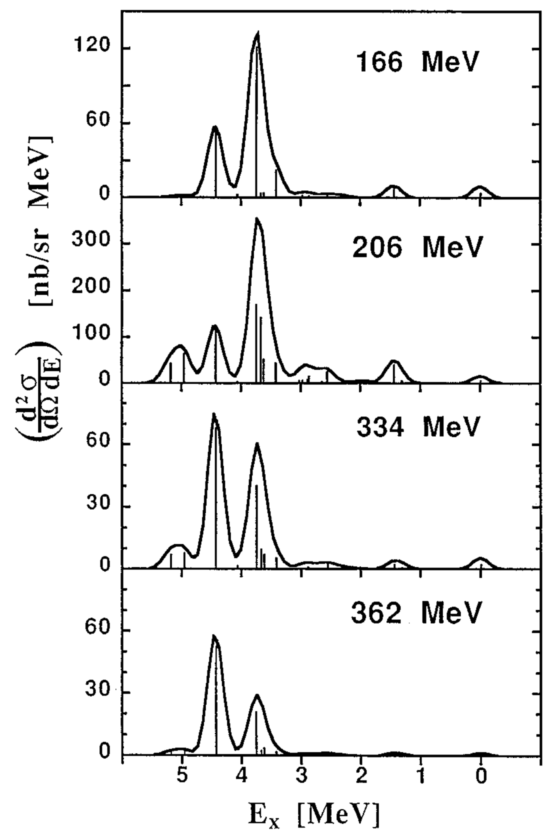

FIG. 4. Calculated spectra for ^{48}Ca$(p,\pi^-)^{49}$Ti at 20° for various incident proton energies. The curves are Gaussian averaged with $\Gamma_{\mathrm{FWHM}}=0.3$ MeV.

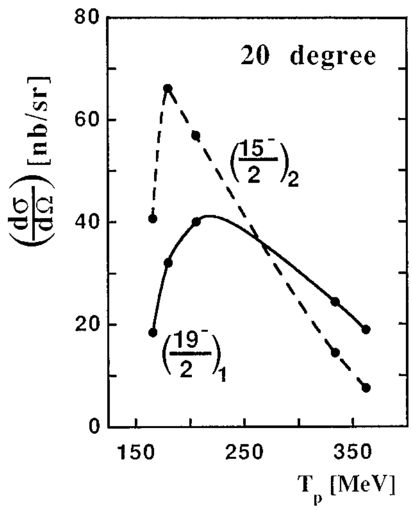

FIG. 5. Reaction cross section for ^{48}Ca$(p,\pi^-)^{49}$Ti leading to final states $(\frac{15}{2}^-)_2$ at $E_x=3.96$ MeV and $(\frac{19}{2}^-)_1$ at $E_x=4.38$ MeV as functions of the incident proton energy.

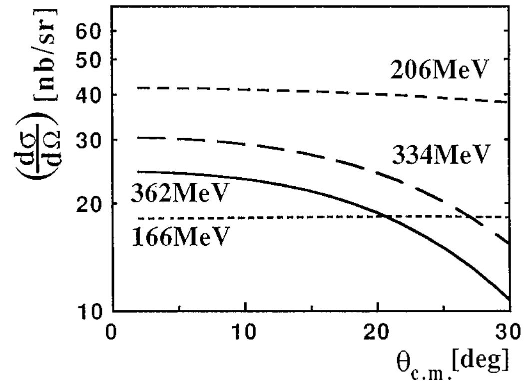

FIG. 6. Reaction cross section of the transition ^{48}Ca$(p,\pi^-)^{49}$Ti$[(\frac{19}{2}^-)_1$:4.38 MeV] for various incident proton energies as functions of the center-of-mass angle.

pect that the reaction cross section has a peak around $T_p \sim 200$ MeV. The decrease of the cross section with the incident proton energy is slower for the $(\frac{19}{2}^-)_1$, which is a maximal high-spin 2p-1h state. In Fig. 6, we show the differential cross section for ^{48}Ca(p,π^-) reactions leading to the $(\frac{19}{2}^-)_1$ state. Obviously, the angular distribution becomes forward peaked with an increase of the incident proton energies due to better momenum matching.

IV. SUMMARY AND CONCLUSIONS

We have carried out the two-nucleon DWBA calculations of the (p,π^-) spectra for calcium isotopes. The experimental data which show the highly selective excitation of low-lying high-spin states are well reproduced by our calculations. The absolute values of the cross sections differ by a factor of 2–3 depending upon the incident energy. The present results indicate that the two-nucleon model succeeds in explaining the overall features of the (p,π^-) reaction in the near-threshold regions without introducing adjustable parameters to fit the (p,π^-) data.

We have also calculated the (p,π^-) cross section near and above the delta resonance considering the availability of a high quality 400 MeV proton facility at RCNP Osaka. For the dominant transitions to the high-spin states, the reaction cross section takes maximal values around the proton incident energy $T_p \sim 200$ MeV. At higher energies, the absolute values of the cross section decrease with an increase of the incident energy. It turned out that the higher-spin states are more selectively excited at higher incident energies. We hope that these results will be checked by further experiments.

We are grateful to Professor S. E. Vigdor for sending us the experimental data on (p,π^-) reactions on Ca isotopes.

[1] S. E. Vigdor, T. G. Throwe, M. C. Green, W. W. Jacobs, R. D. Bent, J. J. Kehayias, W. K. Pitts, and T. E. Ward, Phys. Rev. Lett. **49**, 1314 (1982).
[2] S. E. Vigdor, T. G. Throwe, M. C. Green, W. W. Jacobs, R. D. Bent, J. J. Kehayias, W. K. Pitts, and T. E. Ward, Nucl. Phys. **A396**, 61c (1983).
[3] M. C. Green, J. Brown, W. W. Jacobs, E. Korkmas, T. G. Throwe, S. E. Vigdor, T. E. Ward, P. L. Jolivette, and B. A. Brown, Phys. Rev. Lett. **53**, 1893 (1984).
[4] Z-J. Cao, R. D. Bent, H. Nann, and T. E. Ward, Phys. Rev. C **35**, 625 (1987).
[5] T. G. Throwe, S. E. Vigdor, W. W. Jacobs, M. C. Green, C. W. Glover, T. E. Ward, and B. P. Hichwa, Phys. Rev. C **35**, 1083 (1987).
[6] B. A. Brown, O. Scholten, and H. Toki, Phys. Rev. Lett. **51**, 1952 (1983).
[7] K. Kume, Nucl. Phys. **A504**, 712 (1989).
[8] K. Kume, Nucl. Phys. **A511**, 701 (1990).
[9] K. Kume, Phys. Lett. B **271**, 17 (1991).
[10] H. Toki and K.-I. Kubo, Phys. Rev. Lett. **54**, 1203 (1985).
[11] D. S. Koltun and A. Reitan, Phys. Rev. **141**, 1413 (1966).
[12] O. V. Maxwell, W. Weise, and M. Brack, Nucl. Phys. **A348**, 388 (1980); O. V. Maxwell and W. Weise, Nucl. Phys. **A348**, 429 (1980).
[13] E. Oset and W. Weise, Nucl. Phys. **A319**, 477 (1979).
[14] W. Kutschera, B. A. Brown, and K. Ogawa, Rev. Nuovo Cimento **12**, 1 (1978).
[15] A. Nadasen *et al.*, Phys. Rev. C **23**, 1023 (1981).
[16] D. J. Horen *et al.*, Phys. Rev. C **30**, 709 (1984).
[17] D. Frekers *et al.*, Phys. Rev. C **35**, 2236 (1987).
[18] K. Stricker, H. McManus, and J. A. Carr, Phys. Rev. C **19**, 929 (1979).
[19] K. Stricker, J. A. Carr, and H. McManus, Phys. Rev. C **22**, 2043 (1980).
[20] J. A. Carr, H. McManus, and K. Stricker-Bauer, Phys. Rev. C **25**, 952 (1982).
[21] M. Gmitro, S. S. Kamalov, and R. Mach, Phys. Rev. C **36**, 1105 (1987).